A simulation model for desert runoff and erosion

MIKE KIRKBY

School of Geography, University of Leeds, Leeds, LS2 9JT, UK

Abstract   A distributed hillslope hydrological model is presented
for a slope profile strip of variable width. It is based on stores
representing soil moisture in an irregular bedrock surface, partially
or entirely covered by a colluvial and/or wind-blown regolith. The
model is used to explore the variations in infiltration, overland
flow, soil moisture and evapotranspiration in response to
differences in rainfall totals and storm durations, in gradient and
in regolith depth and uniformity. Infiltration is separately
estimated for bedrock and regolith components with evapotrans-
piration estimated from local soil moisture storage, and therefore
persists longer in areas with only partial regolith cover. Biological
activity is related to storage and evapotranspiration rates. Over-
land flow is routed downslope as a one-dimensional kinematic
wave. The model is also used in aggregate form for longer periods
to estimate erosion by overland flow. Some inferences are drawn
about the extent to which differences between Sde Boker and the
Hovav plateau are due to differences in climate, or to differences
in local relief and in the supply of wind-blown sediment.

BACKGROUND: THE NORTHERN NEGEV DESERT

The work of Yair and his co-workers at sites in the Northern Negev of Israel
at Sde Boqer, the Hovav plateau and near Eilat (Yair & Lavee, 1974, 1985;
Schick, 1977; Yair *et al.*, 1978; Yair, 1983, 1987; Yair & Shachak, 1987) have
established an impressive compilation of data for a set of desert
environments, with detailed information on rainfall distributions over time and
space, overland flow and sediment budgets, together with detailed surveys of
plant and animal activity. Figure 1 shows the distribution of sites, loess cover,
elevation and ancient agricultural fields. Inferences have been drawn *inter alia*
about the influence of biological activity, and about the relationship between
rainfall and sediment yield, given the pronounced increase in wind-blown loess
cover in the wetter (*ca.* 150–200 mm mean annual rainfall) and less rugged
(*ca.* 10 m local relief) areas of the Hovav plateau in comparison to the dryer
(70–100 mm rainfall) and more rugged (*ca.* 25 m relief) Sde Boqer region.
  The simulation model presented here cannot fully represent the inter-
locking complexity of the actual field area; but it concentrates on the slope
hydrology, with a number of simplifying assumptions. The distribution of daily
rainfalls is simulated as an exponential distribution, which provides a good fit
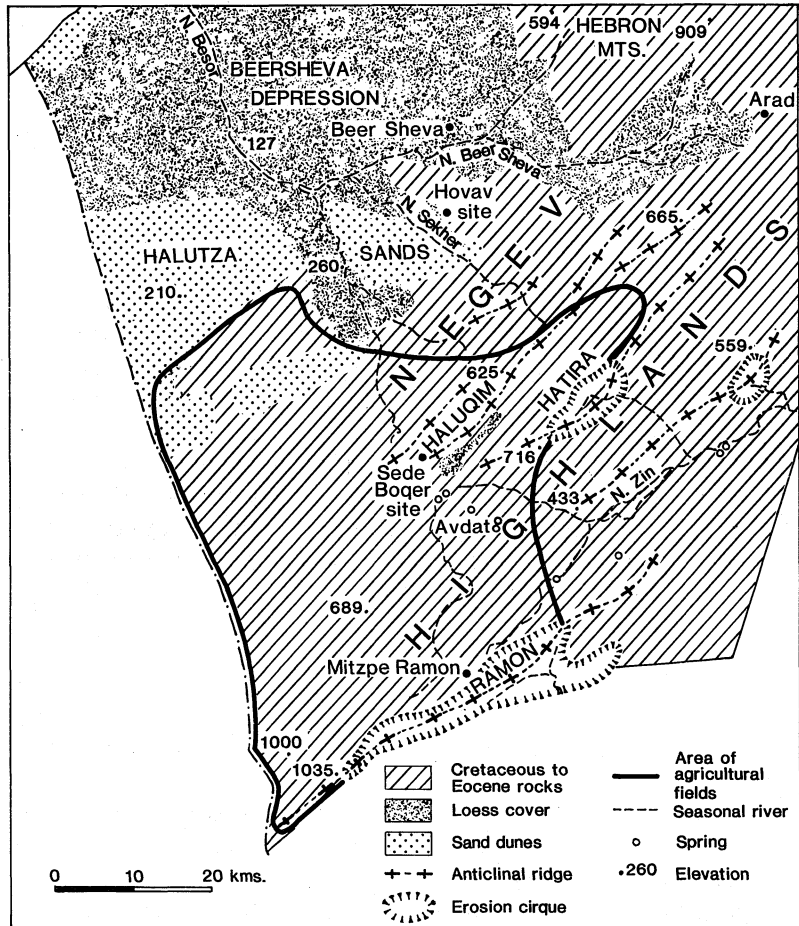for the more frequent frontal storms but may underestimate the importance

Fig. 1 Location map for the northern Negev desert, showing main rock types, areas of loess and sand cover, and area where ancient agricultural fields are found (from Yair, 1987).

of rare and intense convectional storms (Yair & Lavee, 1985). Aspects of the spatial distribution of rainfall (Sharon, 1970, 1980) have been ignored for the individual hillslope strips considered. Within each storm, the distribution of rain showers over time has been estimated from a Markov chain of independent random values. This pattern adequately simulates observed shower sequences and gives peak intensities of up to 20 mm h^{-1} over 3 min periods.

Infiltration, overland flow and evapotranspiration are estimated along a one-dimensional flow strip of variable width, so that two-dimensional flow effects and the location of rilling cannot be identified, unlike the simulation of Dunne & Aubry (1985) for Kenya. Instead the bedrock surface is envisaged as having a statistical distribution of depressions and fissures, giving an explicit relationship between mean regolith depth and proportional regolith cover.

Infiltration is first estimated for the bedrock areas. Excess rainfall from

the bedrock, together with direct rainfall is considered to funnel into the regolith-filled depressions thus providing an increase in potential regolith infiltration. For the low intensity rains normally experienced in the Negev, this concentration leads to greater depths of percolation within the regolith covered proportion of largely rocky areas than occurs in areas with a complete regolith cover. Nevertheless, the total average infiltration is less in the rockier areas, and the overland flow production greater. Evapotranspiration is also estimated separately from rock and regolith proportions of the surface, and is assumed to increase towards a potential rate for high levels of moisture storage. The greater percolation depth in regolith patches leads to a longer persistence of both moisture storage and evapotranspiration. Through these mechanisms, the assumed distribution of bedrock depressions is able to mimic the hydrological responses described by Yair & Shachak (1987).

Overland flow velocities are estimated from flow depth, relying on data presented by Emmett (1978). Flow is routed down slope, taking into account differences in overland flow production resulting from surface composition, and differences in the width of the flow strip. The short duration of individual showers within each rainstorm leads to brief bursts of overland flow which rarely travel more than a few metres downslope before re-infiltrating. Where, as at Sde Boqer, the base of the slope is largely regolith covered (except immediately around the flow collector), there is a much greater overland flow discharge at rocky mid-slope sites than at regolith covered slope base sites. Where, as at sites studied on the Hovav plateau, the whole area is at least thinly mantled with regolith, overland flow is minimal. The results of simulations again mimic the differences observed at the field sites.

During a period between 80 000 and 10 000 years BP, there is evidence for loess accumulation within the Negev area (Yair, 1987). Its present distribution probably follows, to a great extent, original differences in deposition, related primarily to source areas, but also by differential washing out of wind carried dust by rainfall. The distribution may also, in part, reflect subsequent differences in erosion rates. Differential washing out and differential erosion may be partly responsible for the greater loess cover in the wetter lowland areas to the north, including the Hovav plateau site, compared to the dryer and more rugged areas to the south. The simulation model allows loess deposition, and erosion by rainsplash and wash, to proceed concurrently or in turn, so that the factors of topography, rainfall and loess deposition rates may be investigated independently. This provides some test of the inferences drawn by Yair (1987) and Yair & Shachak (1987) about the relationship between rainfall and sediment yield for the Negev area.

MODEL FORMULATION

The simulation requires formal specification of macro- and micro-topography, rainfall, infiltration, overland flow, evapotranspiration and sediment transport. These specifications are set out briefly below.

The macro-topography is based on the general features of the Sde Boqer site, and in particular on plot 2, A-C, shown in Fig. 2. The simulated slope is
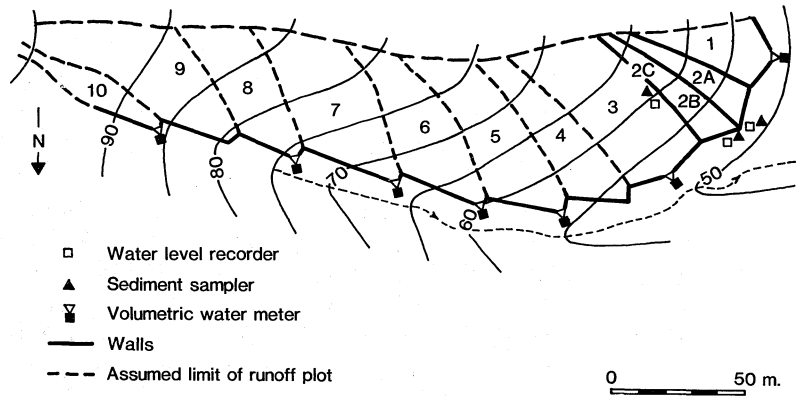
Fig. 2   *Sde Boqer Field plots 1-10 (from Yair, 1987).*

shown in Fig. 3, with a near uniform gradient and a linear increase in regolith cover downslope, from 0% at the divide to 70% cover at the base (Fig. 4). The general widening of the strip has been included but not the detailed form of the divide nor the basal narrowing towards the runoff collectors at the lowest point. It should also be noted that the small area of bedrock immediately surrounding the collectors has not been included in the simulation.

The micro-topography has been simulated by assuming that the proportion $p(z)$ of the area depressed more than a depth z below local highs is given by:

$$p(z) = \exp(-z/z_0) \tag{1}$$

for a mean depth z_0, which has been taken as 250 mm in most simulations. This distribution implies the existence of some deep fissures but no high pinnacles. If this pattern of depressions is filled to an average depth z_1 with regolith material, then the proportion of soil cover is simply z_1/z_0 or 1.0, whichever is less. The depressions are then filled to within a depth of $z_0 \ln(z_0/z_1)$ of the local highs (for $z_1 < = z_0$), or the highs are buried to depth $z_1 - z_0$ (for $z_1 > = z_0$).

The distribution of daily rainfalls has also been taken as exponential, with the number of rains exceeding r given by:

$$N(r) = N \exp(-r/r_0) \tag{2}$$

where N is the mean annual number of rain days, and r_0 is the mean rain per rain day (= Mean Ann. Rf/N). This distribution has been successfully fitted for a range of climates and time periods, provided there is not strong seasonality. For a 32 year period, the Sde Boqer site averaged 93 mm, ranging from 34 to 167 mm, falling on 15 to 42 days. For the simulation, an average of 93 mm was used over an average of 25 days per year. A random 32 year period gave a range of 54 to 170 mm, falling on 19 to 35 days, showing adequate agreement.

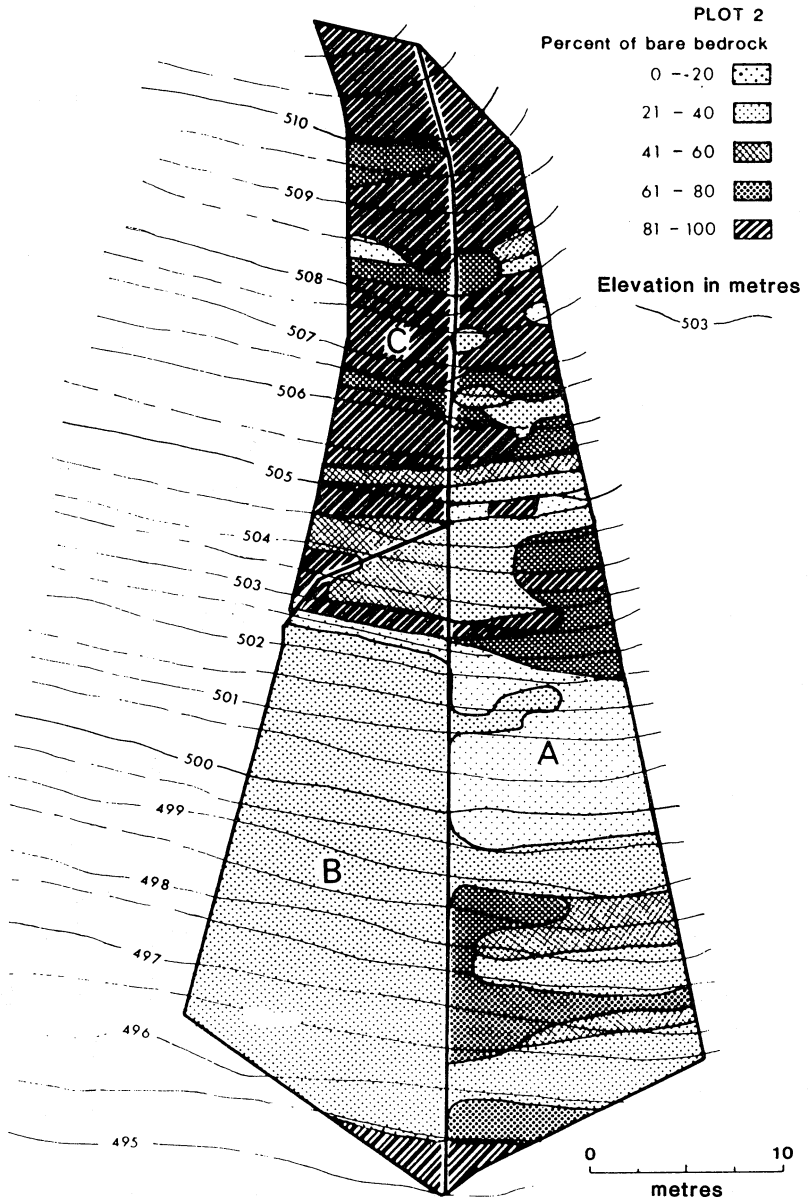Within storms, the pattern of rain showers has been simulated using a

Fig. 3 *Sde Boqer field plots 2 A-C, showing the proportion of bare bedrock and plot boundaries (from Yair & Lavee, 1985).*

first order Markov chain with 50% persistence, so that each value is the mean of the previous value and a random variable. The random variable is obtained from a normal distribution with zero mean, using the positive values and replacing the negative values by zeros. The variance of this distribution is adjusted to give the required mean of approximately 2 mm h^{-1} overall. Figure 5 illustrates some simulated 20 mm storms showing the shower pattern produced. It may be compared with the actual storms
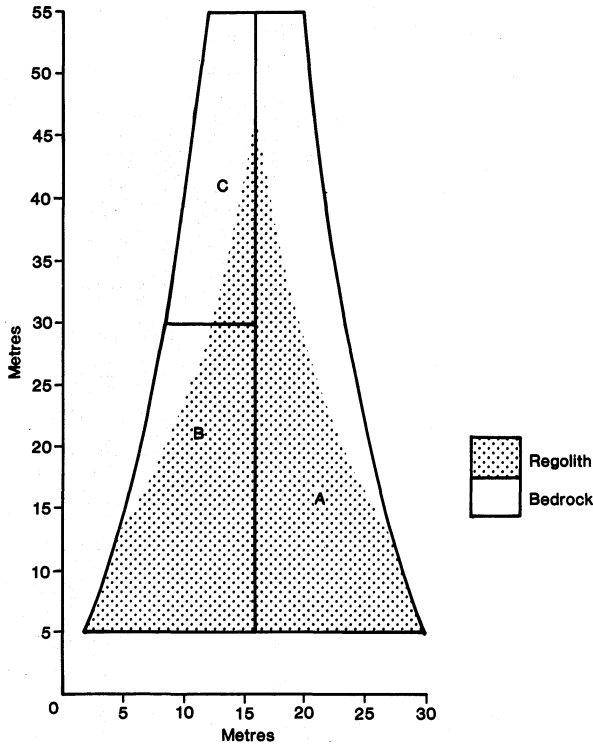
Fig. 4 Simulated flow strip map showing proportions of bedrock and regolith, modelled on plots shown in Fig. 3.

illustrated in Fig. 6. Figure 7 shows the distribution of storm amounts and durations. It may be seen that the extreme storms contained in Fig. 6 lie outside the scatter of points, showing that the simulation provides a narrower grouping than that actually observed, and that the 50% persistence should be increased.

Infiltration capacity has been calculated using the Green & Ampt (1911) equation of the form:

$$f = f_0 + B/S \tag{3}$$

where S is a water storage level; and f_0, B are constants.

This formulation is consistent with the Philip (1957, 1958) time-based infiltration equation:

$$f = f_0 + (B/2)^{1/2} \, t^{-1/2} \tag{4}$$

for an initially dry soil. The near-surface storage level S is increased by rainfall, and simultaneously decreased by the steady infiltration rate, f_0, which is added to a percolation store, P. Then for infiltration under rainfall at a steady intensity i ($> f_0$), the time to ponding is given by:
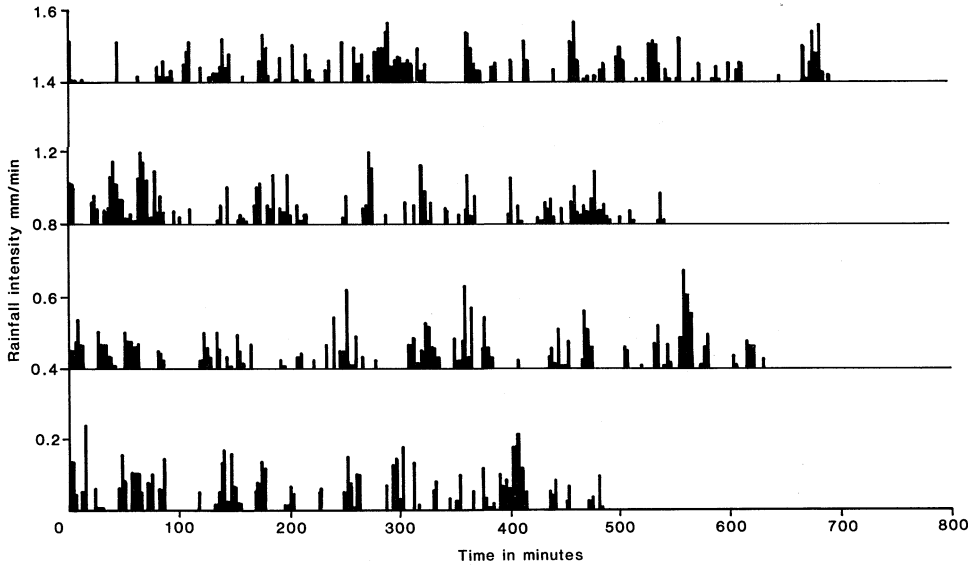
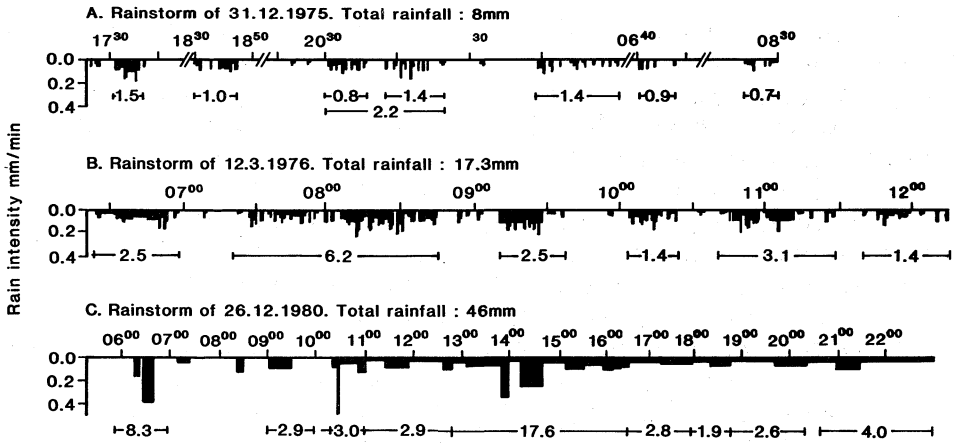***Fig. 5*** *Four 20 mm rain storms simulated by 3 min units.*

Fig. 6 *Three natural frontal rain storms for the Sde Boqer area (from Yair, 1987).*

$$t_0 = B/(i - f_0)^2 \tag{5}$$

The values used in this simulation are:

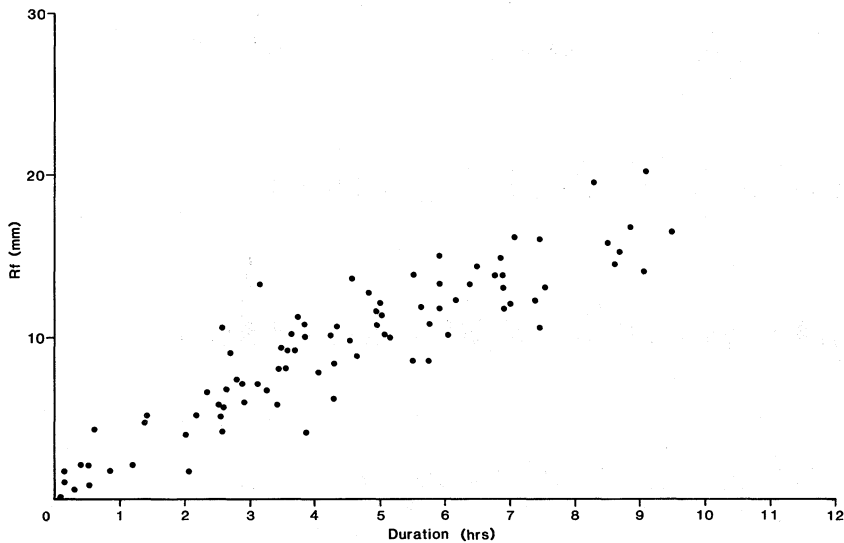|	f_0(mm h^{-1})	B(mm^2 h^{-1})
Bedrock	0	2.4
Regolith	10	24

Fig. 7 The scatter of simulated rain storm amounts and durations.

Figure 8 shows simulated infiltration rates for bedrock and regolith. In comparison to measured rates under a simulated rainfall of 26 mm h^{-1}, (Fig. 9), the bedrock infiltration rate shows the limitation of an equation of the above type, although there is an adequate fit to the regolith data. The forecast initial rate is too low, and the rate after 10 minutes or more is too high. Figure 10 shows the effect of a simulated 30 min storm of 26 mm h^{-1} on flow strips similar to Sde Boqer, plots 2B and 2C. For the rocky slope there is little runoff for the first 3 min, indicating an effective threshold capacity of 1.3 mm before runoff; for the regolith slope the threshold capacity is 6.5 mm. These compare with observed runoff thresholds of 1–3 and 3-5 mm respectively, so that the simulated values are considered satisfactory.

In low intensity rains, the amount of water infiltrated into areas which are partially regolith-covered is higher than a weighted average of the amounts infiltrated into rock and soil separately. This is because water running off the rock is allowed to funnel into the regolith areas and infiltrate. Nevertheless the total infiltration is less than for areas completely covered with regolith, and the overland flow production is greater.

Overland flow velocities have been estimated using Emmett's (1970) data, although these show little pattern other than a general increase of mean velocity with flow depth. The theoretical exponent of depth to give flow velocity should be 2/3 for turbulent flow and 2 for laminar flow. The data suggest that a value of 1.0 provides a tolerable fit, and that there is little evident dependence on slope gradient. The relationship:

$$v = 10 \, d \tag{6}$$

has therefore been adopted, where v is the mean velocity in m s^{-1} and d is the mean flow depth in m. The kinematic wave velocity should be exactly
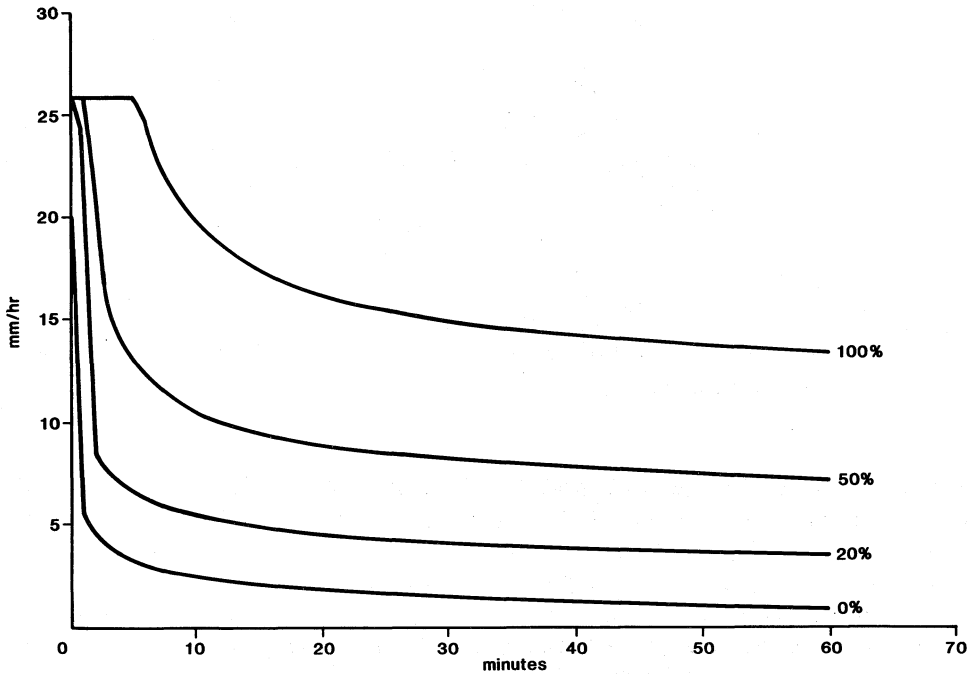
Fig. 8 *Simulated infiltration rates during rainfall at 26 mm h⁻¹ into slopes of differing regolith cover.*

···· Rocky slope
— Colluvial slope (dry surface)
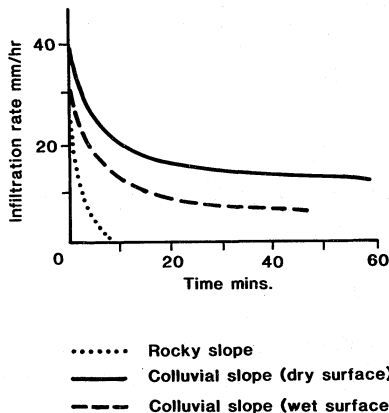– – – Colluvial slope (wet surface)

Fig. 9 *Measured infiltration rates during artificial rainstorm at 26 mm h⁻¹ on bedrock and colluvium covered surfaces (from Yair & Shachak, 1987).*

twice this value. For a flow of $1 \ l \ s^{-1} \ m^{-1}$, this relationship gives a flow depth of 10 mm at a mean velocity of $0.1 \ m \ s^{-1}$.

Overland flow has been routed downslope along the variable width flow strip as a kinematic cascade, using 3 min iterations over 2.5 m distance increments until flow and rainfall come to an end. This part of the model is very similar in principle to that described by Yair & Lavee (1985). For the
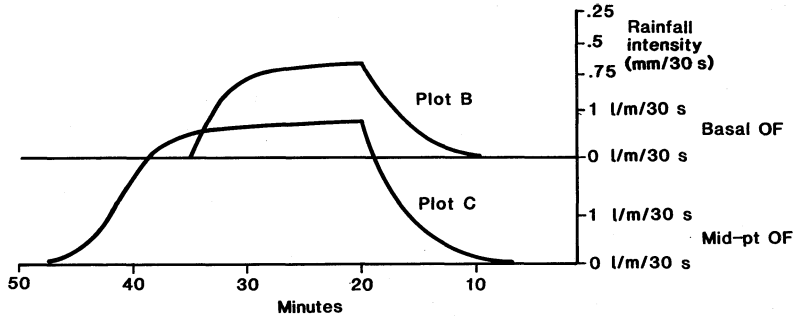
Fig. 10 *Simulated runoff from plots B and C for a 30 min rainstorm at 26 mm h^{-1}.*

remainder of each rain day, and for days without rainfall, evaporation is integrated over the whole of the relevant period. For convenience, and without significant loss of accuracy for an arid area, rain storms are invariably simulated at the start of each water day on which they occur.

Evapotranspiration (ET) is estimated for bedrock and regolith proportions of the surface at each point. It is calculated for each 3 min increment during storm events and integrated over the remainder of rain days, and for dry days as a whole. Actual ET is estimated from a potential rate e_p (assumed to be 5 mm per day). Losses are taken at the potential rate from any overland flow layer and from the near-surface store until both are exhausted. Subsequently, the actual rate is taken as a function of the percolation storage P, at rate:

$$e_p [1 - \exp(-P/P_0)] \tag{7}$$

where P_0 is a scale depth for the rate of attenuation. Integrating this over a period Δt, the total loss is:

$$P - P_0 \ln\{1 + [\exp(P/P_0) - 1]/\exp(e_p \Delta t/P_0)\} \tag{8}$$

where P is the percolation storage at the beginning of the period.

Because, in low intensity rains, more water enters the percolation store in areas of partial regolith cover, it follows that the ET lasts longest at these sites, and is greater per unit area of regolith. An even more favourable environment is provided at sites where regolith cover is increasing downslope, especially close to a sharp boundary, because overland flow generated upslope re-infiltrates preferentially, so that the total ET and not only the ET per unit area of regolith, is increased. In favourable sites, simulations suggest that the total ET may be 25–35% greater than the rainfall.

Although biological components are not explicitly included in this model, an estimate of density for vegetation cover, and for soil fauna depending on it may be obtained as follows. Suppose the mean actual ET is AE in an area with a proportion p of regolith cover; and that the required ET per unit area to support a vegetation type is RE (perhaps 25% of the potential ET).

Accordingly, in the area of adequate unit ET, that is where $AE/p > RE$, the relative density is proportional to p. In the area of insufficient ET however, the density is proportional to $p[AE/(pRE)]^m$, for an exponent $m > 1$ (for the sake of illustration let $m = 4$). A power law gives continuity at the cross-over point, at which the regolith proportion p is equal to the ratio AE/RE, and expresses the probability of a pocket of locally concentrated soil moisture.

The final component of the model is sediment transport by wash and splash processes. Rainsplash is estimated as proportional to the square of the rainfall intensity, and is considered to occur only on regolith covered parts of the surface. Wash is estimated as proportional to the square of the overland flow discharge, and a relationship of this kind is supported by some sediment data for the Sde Boqer site (Fig. 11). In this case the concentration of regolith areas in depressions has two opposing influences. First, it may lead to flow concentration within the depressions, depending partly on their orientation; and second the depressions may provide local reverse slopes which hinder sediment evacuation, particularly for low proportions of regolith cover, at which the regolith material is concentrated in fissures. As a compromise the rate of wash transport has been taken as proportional to the square root of proportional regolith cover, so that large amounts of cover give little attenuation, and *vice versa*.

Both splash and wash have been estimated as directly proportional to gradient, and no lower threshold for wash has been set, as seems appropriate for wind deposited material (although a substantial threshold would be
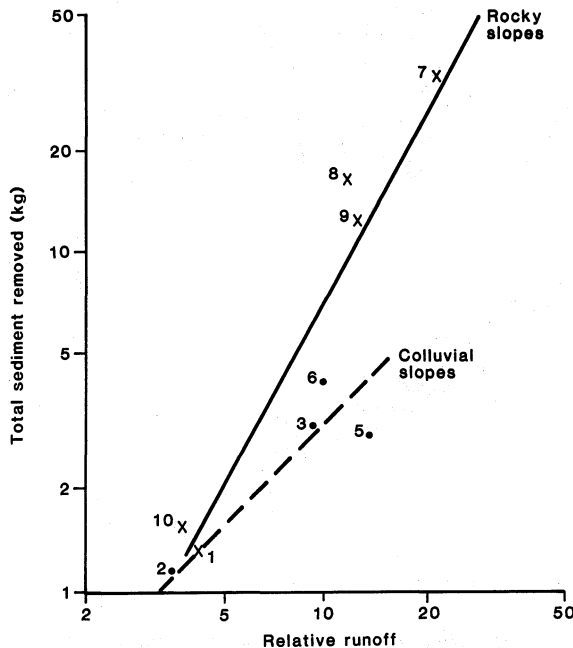

Fig. 11   Total sediment transport and total plot runoff (as % of combined plot runoff) for Sde Boqer plots, for the year 1972–1973 (data from Yair & Shachak, 1987).

appropriate for stony colluvial material). A balance between wash and splash rates has been arbitrarily chosen to give dominance to wash in areas of significant overland flow. The balance between these processes and rates of sediment supply, either as wind-blown loess or by weathering of bedrock as a source of colluvium, has been varied in order to examine the effect of differing ratios of supply to removal in the location of the regolith cover. In order to span from the hydrological simulations of a few years up to relevant periods for erosion and deposition of a few thousands of years, each year's sediment yields have been multiplied by a replication factor of 50 to 200 to provide detectable changes in the distribution of soil cover. Even for these time spans however, no erosion of the bedrock surface has been included in the simulation.

SIMULATION RESULTS

Figure 12 illustrates a number of the features of the simulated hydrographs and sediment yield for a 50 m plot with bedrock exposed for the top quarter
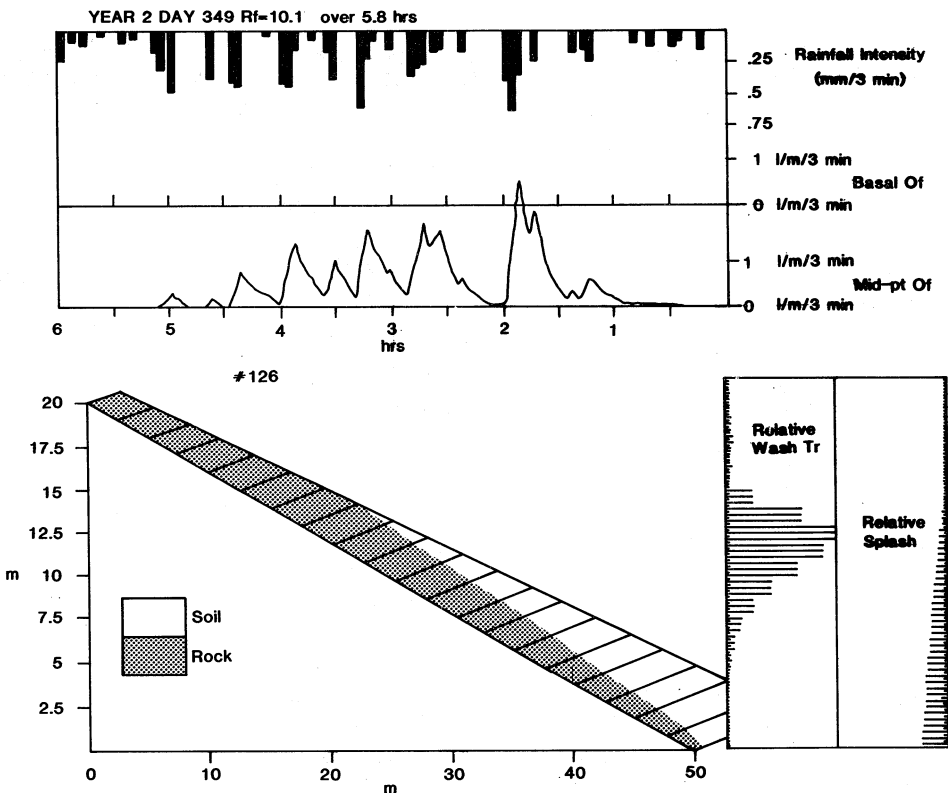

Fig. 12 Simulated example hydrograph from plot A, for the slope profile form shown. The relative cumulative magnitudes of sediment transport by rainsplash and wash down the slope length are also shown.

of the slope, and regolith cover then linearly increased to 90% at the slope base. It may be seen that there is a substantial response to rainfall at mid-slope sites, but little from the regolith areas at the foot of the plot. In comparison with Sde Boqer, the mid-slope flows are of the correct order of magnitude; but the slope base flow is much less than from the field plot, probably because of the rocky area immediately above the slope-base collector. The rain showers are brief enough, even on the relatively short 50 m slopes, and show an appreciable increase in flow downslope only within rocky areas. Figure 13 shows annual overland flows for the configuration shown in Fig. 12, with a pronounced peak at the foot of the rocky area. The accumulation downslope may be compared with flows along a completely rocky slope, where about 70 m is required to reach equilibrium discharge, and on a slope with 15% regolith cover where greater infiltration produces equilibrium within about 20 m as well as greatly reduced total flows.

Figure 12 also shows the pattern of sediment transport rates forecast from the flow and rainfall data for this profile of almost uniform gradient. It may be seen that splash rates increase steadily downslope, largely reflecting the increased proportion of regolith cover downslope. Wash rates, on the other hand, show a marked peak (at 22 m from the crest), somewhat downslope from the overland flow peak (at 17 m) because of the increasing availability of sediment in a downslope direction.

Over a period, the effect of this sediment transport peak is to "sweep" sediment downhill, especially in the area near the top of the regolith. Figure
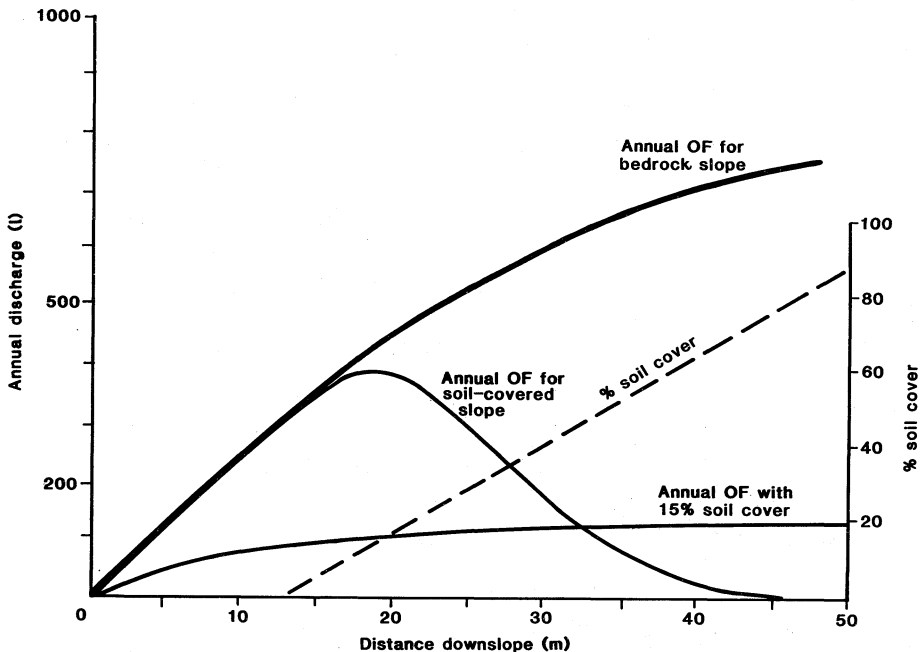

Fig. 13   Simulated annual overland flow discharge for slopes of constant regolith cover, and for slopes with regolith cover increasing downslope as indicated.

14 shows a simulation in which an initially bedrock-surfaced slope is subjected to loess deposition at a rate increasing from zero at the hill crest to 60 mm per 1000 years at the slope base. It may be seen that a thin, patchy equilibrium cover is established progressively from the crest downwards. Near the slope base, given the basal conditions used, net deposition is close to the input rate. In the middle third of the slope, however, there is a transition, which becomes more abrupt with time, from a mainly bedrock slope to a mainly regolith covered slope.

In this way, sediment can be effectively swept downslope in areas where there is a balance between loess input and sediment transport capacity. In areas of relatively higher loess input, the sweep effect is slight and the sweep zone migrates upslope, whereas in areas of relatively lower loess input, the sweep zone migrates downslope until, in extreme cases, the entire deposit is removed. In the transect from north to south across the northern Negev, the field evidence thus suggests that the influence of high deposition rates and low gradients in the north outweighs the effect of greater rainfall and allows loess to cloak the landscape. In the south, the low deposition rates and steep gradients similarly appear to be more important in preventing loess accumulation than the influence of low rainfall in reducing erosion. At Sde Boqer, the combination of rocky hillslopes and loess-filled valleys appears to be much closer to the critical balance.

The effect of erosion sweeping of loess can also be seen in annual ET and storage estimates. Figure 15 shows the same time sequence as in Fig. 14 for mean ET rates. There is some slight scatter produced by using data from
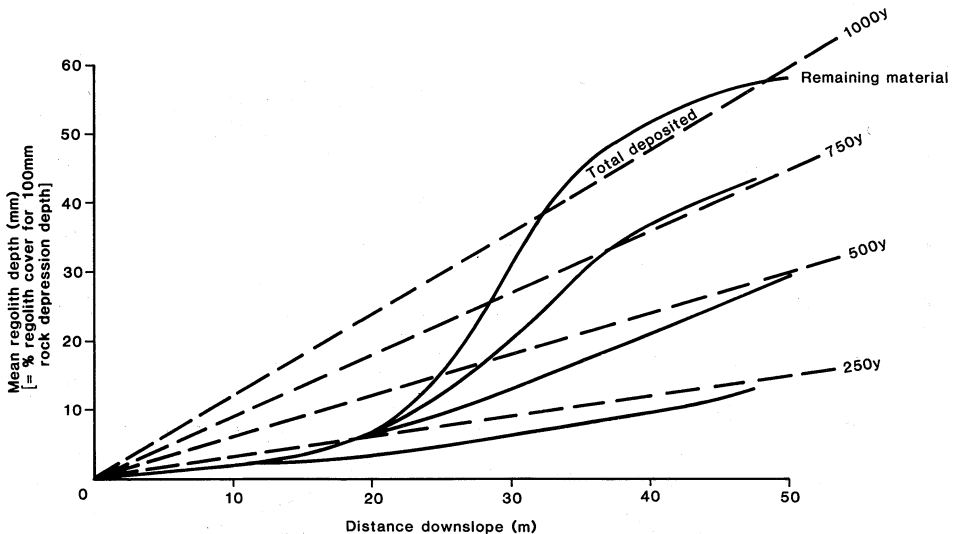

Fig. 14   Simulated course of total deposition (straight lines) and net soil cover, including the effects of deposition and sediment transport. Loess deposition increases linearly downslope to 60 mm per 1000 years at the slope base. The effect of sediment sweeping may be seen.
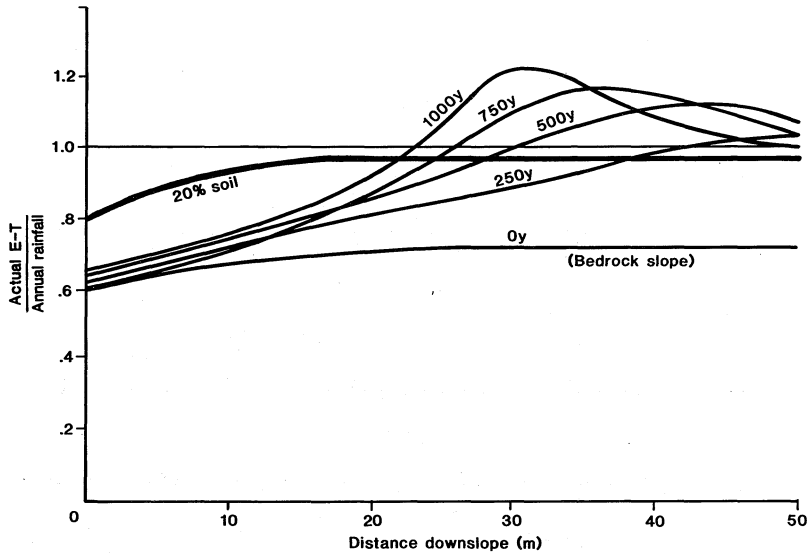
Fig. 15 Enhancement of simulated mean annual evapotrans-piration by erosion "sweeping". The time sequence refers to the same run as in Fig. 14.

particular years with higher or lower total rainfall, but a clear pattern is evident. For comparison the influence of uniform loess deposition is also indicated. The sweep effect is responsible for bringing mean rates above the rainfall in the zone of declining overland flow. Overland flow re-infiltrates into the loess in the sweep zone, producing a progressively sharper peak in soil water storage and ET. In this example the mean ET is about 20% greater than the rainfall, and in some runs this enhancement rises to over 30%.

Some estimate of relative plant density may be inferred from these evapotranspiration data as described above. In Fig. 16, the same sequence has again been used for illustration. Local ET in rainfall patches has been estimated as the ratio of mean ET to proportion of rainfall cover, and a critical value of 450 mm (approximately 25% of the assumed annual potential ET of 1825 mm) has been arbitrarily chosen as the threshold level for the growth of perennial plants and the establishment of associated herbivores. In the area of inadequate local ET, a fourth power law has been used to sketch the decline in density. Slopes of constant loess cover have also been included for comparison. The densities referred might best be identified, *a priori*, with root spread densities: crown covers are likely to be half as great, or even less.

In the simulation, the most favourable uniform slope for biological activity appears to be one with about 20% regolith cover, with sharp reductions in density on either side of this optimum. During the simulated evolution of the regolith cover, as sediment is swept downslope, there is a narrow zone of maximum biological activity, which may be locally richer than for the best uniform slope. On either side of this maximum, biological activity declines sharply; upslope, because of a shortage of regolith sites, and
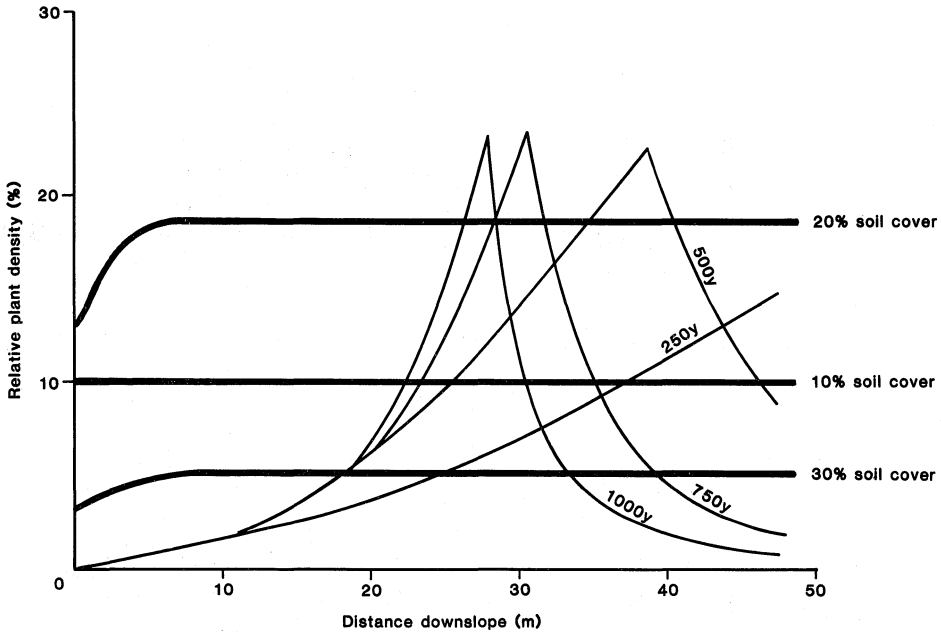
Fig. 16 *Estimated relative plant densities (perhaps related to root cover), estimated from simulated hydrological data, for uniform rainfall covers and for the erosion and deposition sequence shown above.*

downslope because of a lack of water within rooting depth. When the distribution of annual rainfalls is taken into account, the sharpness of this peak is somewhat softened, so that the apparent local advantage may be less narrowly confined. It may also be seen that as soil cover increases over time, the breadth of the favoured area for plants tends to become narrower as it migrates upslope.

CONCLUSIONS

Some tentative conclusions may be drawn from the simulation about the relationship between sediment yield and rainfall in this arid environment, and about the nature of the relationship between biological activity and sediment yield.

In estimating sediment yields, no account has been taken of the possible effects which are commonly thought to control Langbein & Schumm's (1958) well-known relationship. In particular, no account is taken of the influence of vegetation crown cover in shielding the surface from the effects of rainsplash and crusting, nor of improved infiltration capacity in response to increases in soil organic matter. In addition, no consideration has been given to increased flow resistance from vegetative roughnesses. For the densities considered in the simulation, and observed in the field, it is argued that these effects can be

largely ignored in the range of rainfalls and vegetation covers involved, at least up to about 200 mm annual rainfall. The maximum root density is estimated, for optimum loess cover, at about 40%, with corresponding crown cover of 20% or less. Given the short showers which make up most of the rainfall, the effect of increased rainfall should be an almost linear increase in both wash and splash erosion, with the main difference in the frequency of flows rather than in their peak discharge. Thus the overall response to increasing rainfall, for a given degree of loess cover, is seen as a clear, and almost linear, increase in sediment yield. The most important possible counter argument is that the rate of loess deposition is causally linked to rainfall, through scrubbing out of wind blown dust by the rain.

Another conclusion from the simulation is that plant and animal densities, as well as the spatial pattern of sediment transport, can both be explained as depending on the slope hydrology. Figure 17 shows a fairly clear empirical relationship between actual sediment yield and biologically available material, but it is plain, from the contrast between plots with a colluvial footslope and those in bedrock, that other and presumably hydrological factors are at least as important as biological disturbance. It is therefore argued that there need not be a cause and effect relationship between biological activity and erosion, but that both may primarily be independent responses to the hydrological regime.
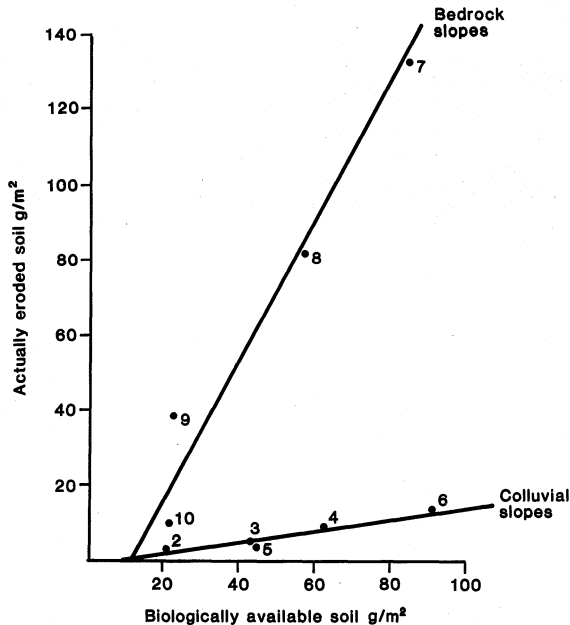

Fig. 17 Empirical relationship between soil actually eroded and biologically "available" material, for the 8 mm storm of 24 November 1972 on Sde Boqer plots (data from Yair & Shachak, 1987). Note the strong distinction between bedrock plots and those with a colluvial base.

Acknowledgement   I would like to thank Aaron Yair for this advice and support, and for providing the data which are referred to in this paper.

REFERENCES

Dunne, T. & Aubry, B. F. (1985)   Evaluation of Horton's theory of sheetwash and rill erosion on the basis of field experiments. In: *Hillslope Processes* (ed. A. D. Abrahams), 31-53. Allen & Unwin, Boston, Massachussetts, USA.

Emmett, W. W. (1970)   The hydraulics of overland flow on hillslopes. *USGS Prof. Pap.* 662A.

Emmett, W. W. (1978)   Overland Flow. In: *Hillslope Hydrology* (ed. M. J. Kirkby) 145-176. John Wiley, Chichester, UK.

Green, W. H. & Ampt, G. A. (1911)   Studies in Soil Physics. 1: The flow of air and water through soils. *J. Agric. Sci.* 4 (1), 1-24.

Langbein, W. B. & Schumm, S. A. (1958)   Yield of sediment in relation to mean annual precipitation. *Trans. AGU* 39, 1076-1084.

Philip, J. R. (1957, 1958)   The theory of infiltration. *Soil Sci.* 83, 345-357 & 435-448; 84, 163-177, 257-264 & 329-339; 85, 278-286 & 333-337.

Sharon, D. (1970)   Areal patterns of rainfall in a small watershed. In: *Symposium on the Results of Research on Representative and Experimental Basins,* (Wellington 1970), Vol. I, IAHS Publ. no. 96, 3-11.

Sharon, D. (1980)   The distribution of hydrologically effective rainfall incident on sloping ground. *J. Hydrol.* 46, 165-188.

Schick, A. P. (1977)   A tentative sediment budget for an extremely arid catchment in the southern Negev. In: *Arid Geomorphology* (ed. D. O. Doehring), 139-163. Publications in Geomorphology.

Yair, A. (1983)   Hillslope hydrology, water harvesting and areal distribution of ancient agricultural fields in the northern Negev desert. *J. Arid Environ.* 6, 283-301.

Yair, A. (1987)   Environmental effects of loess penetration into the northern Negev desert. *J. Arid Environ.* 13, 9-24.

Yair, A. & Lavee, H. (1974)   Areal contribution to runoff on scree slopes in an extreme arid environment: a simulated rainstorm experiment. *Z. Geomorphol. Suppl. Bd.* 21, 106-121.

Yair, A. & Lavee, H. (1985)   Runoff generation in arid and semi-=arid zones. In: *Hydrological Forecasting* (ed. M. G. Anderson & T. P. Burt), 183-220. John Wiley, Chichester, UK.

Yair, A. & Shachak, M. (1987)   Studies in watershed ecology of an arid area. In: *Progress in Desert Research* (ed. L. Berkofsky & M. G. Wurtele), 145-193. Rowman & Littlefield, Totowa, New Jersey, USA.

Yair, A., Sharon, D. & Lavee, H. (1978)   An instrumented watershed for the study of partial area contribution of runoff in the arid zone. *Z. Geomorphol. Suppl. Bd.* 29, 71-82.